

Effects of annealing on infrared and thermal-effusion spectra of sputtered *a*-Si:H alloys

G. Talukder, J. C. L. Cornish, P. Jennings, G. T. Hefter, and B. W. Clare
School of Mathematical and Physical Sciences, Murdoch University, Murdoch, WA 6150, Australia

J. Livingstone
Department of Electrical and Electronic Engineering, University of Western Australia, Nedlands, WA 6009, Australia

(Received 2 January 1991; accepted for publication 23 September 1991)

Infrared spectroscopy and thermal effusion have been used to study the nature of the silicon-hydrogen bond in sputtered *a*-Si:H alloys. The samples were prepared by reactive sputtering under different deposition conditions to produce varying hydrogen contents. The Fourier transform infrared spectra have been analyzed using the simplex algorithm to deconvolute the component peaks. This technique has been applied separately to both the stretching- and bending-mode regions of the infrared absorption spectra. Studies have been made of the effects of annealing on both the infrared and the thermal evolution spectra of hydrogen. The results indicate a redistribution and transformation of different bonding configurations due to annealing. A comparative study is presented of the thermal-effusion spectra for partial and total degassing with the infrared spectra taken before and after each phase of degassing.

I. INTRODUCTION

The role of hydrogen in hydrogenated amorphous silicon (*a*-Si:H) has been extensively studied over the last 10–15 years.^{1–6} It is believed that the quality of an *a*-Si:H alloy is closely related to its hydrogen content and to the nature of the silicon-hydrogen bonds. For these reasons we have characterized our samples by: (i) infrared vibrational spectroscopy to provide information about the bonding configuration and the total hydrogen content and (ii) thermal evolution (TE) spectroscopy to investigate the atomic distribution of hydrogen in the amorphous silicon network and the mechanism of its release.

a-Si:H films often contain a significant amount of unintentionally incorporated impurities such as oxygen, nitrogen, etc. Such impurities, when present even in small concentration, can significantly influence the optoelectronic properties of *a*-Si:H films. For example, Tsai, Stutzmann, and Jackson⁷ have shown that in *a*-Si:H films, the light-induced spin density is influenced by the presence of oxygen and nitrogen with concentrations exceeding the values of 0.2 and 0.02 at. % respectively. Carlson *et al.*⁸ have also observed some light-induced changes in the ir absorption spectra associated with the presence of oxygen in the *a*-Si:H films. Street⁹ has shown that thermally induced changes in the density of states, the light-induced changes known as the Staebler–Wronski effect,¹⁰ and some other reversible metastable changes occurring in *a*-Si:H films have common origin. Hence, it was felt worthwhile to study the effect of annealing on the ir and TE spectra for *a*-Si:H films slightly contaminated with oxygen and nitrogen.

In the production of solar cells and in many other applications, the *a*-Si:H thin film forms only part of the device and is likely to undergo further heat treatment and/or deposition. In subsequent use, solar cells in particular may be subjected to radiation and temperature cycling over

a wide range of temperatures. Hence it is necessary to investigate the changes that may occur during such treatments. In the present work we have investigated the changes that occur in the infrared absorption and thermal-effusion (TE) spectra due to annealing at temperatures ranging from ~250–450 °C. Although sputtered *a*-Si:H films do not produce good solar cells, we have studied such samples for the following reasons. The ir absorption spectra of samples produced by reactive sputtering^{2,3} and glow discharge decomposition of SiH₄^{11,12} show essentially the same features. The reactive sputter deposition method has the advantage that the hydrogen content of the films can be independently controlled by adjusting the hydrogen partial pressure in the discharge. An understanding of the structure and properties may indicate why sputtered *a*-Si:H is not a very good photovoltaic material.

Fritsche¹³ and Beyer and Wagner¹ found, for their samples prepared by glow discharge (GD), that hydrogen evolution takes place mainly at two temperatures: ~400 and 600 °C. However, Biegelsen *et al.*¹⁴ claim that they have found an intermediate peak as well for their GD samples. On the other hand, a variety of TE spectra have been reported for samples prepared by reactive rf sputtering.^{15,16}

There have been some studies of *a*-Si:H using both ir absorption and TE,^{1,4,16–18} but a comprehensive study to investigate the effects of annealing on the corresponding spectra of *a*-Si:H films with trace contamination by oxygen and/or nitrogen has not previously been reported.

II. EXPERIMENT

The sample preparation and characterization techniques used in this study have been described previously.¹⁹

The Fourier transform infrared (FTIR) spectra have been analyzed following the use of a computer program based on the simplex algorithm for the deconvolution of the component peaks. This technique has been applied sep-

arately in the stretching and the bending-mode regions of the ir absorption spectra to decompose each region into its component peaks. The stretching band has been deconvoluted into two Gaussians with centers at 2000 and 2090 cm^{-1} . Whereas, the bending band has been deconvoluted into four component peaks with centers at 790, 845, 890, and either 940 or 980 cm^{-1} depending on the type of impurities present in the sample under consideration.

Our samples ranged from those with no detectable impurities, to some contaminated with oxygen, with nitrogen, or both. A small leak in the system provided the source of the gases and the proportion of each gas in the film depends on the deposition conditions.

The integrated intensity under a particular peak, in the ir absorption spectrum, was deduced using the following formula:²⁰

$$I_{ij} = \int \frac{\alpha(w)}{w_0} dw, \quad (1)$$

where I_{ij} , α , w , and w_0 are the integrated absorption, the absorption coefficient, the wave number, and the peak wave number, respectively. We have used $i = \text{H, N, or O}$ for hydrogen, nitrogen, and oxygen, respectively, and $j = \text{W, B, and S}$ for the wagging, bending, and stretching modes of vibration, respectively. The hydrogen, nitrogen, and oxygen concentrations were deduced using the equation

$$C_i = A_{ij} I_{ij} \quad (2)$$

where C is the concentration, A is the proportionality constant, and I is the integrated intensity defined by Eq. (1). We have used $A_{HW} = (1.6 \times 10^{19} \text{ cm}^{-2})$ (Ref. 20) for the Si-H wagging mode at 650 cm^{-1} , $A_{OS} = (2.8 \times 10^{19} \text{ cm}^{-2})$ ^{3,17,21} for the Si-O stretching modes, and $A_{NS} = (2.9 \times 10^{18} \text{ cm}^{-2})$ ²² for the Si-N stretching modes.

The oscillator strength for the Si-H stretching mode Γ_{HS} was calculated using the formula²⁰

$$\Gamma_{HS} = 37.6 (I_{HS}/I_{HW}) \text{ cm}^2/\text{mmol}, \quad (3)$$

where I_{HS} and I_{HW} are the integrated intensities of the stretching and wagging bands, defined by Eq. (1), respectively.

III. RESULTS AND DISCUSSIONS:

A. Infrared absorption spectra of as-deposited samples

The ir absorption spectrum for a typical sputtered a -Si:H film has been shown and its hydrogen-related features have been described elsewhere.¹⁹ For the slightly contaminated samples, the oxygen- and nitrogen-related features are described briefly in the following sections.

B. Infrared absorption spectra of annealed samples

1. High-temperature annealing ($T_a > 300^\circ\text{C}$)

Figures 1(a), 1(b), and 1(c) show the ir spectra for the Si-H wagging, bending, and stretching vibration modes, respectively, for a sample containing ~ 23.8 at. %

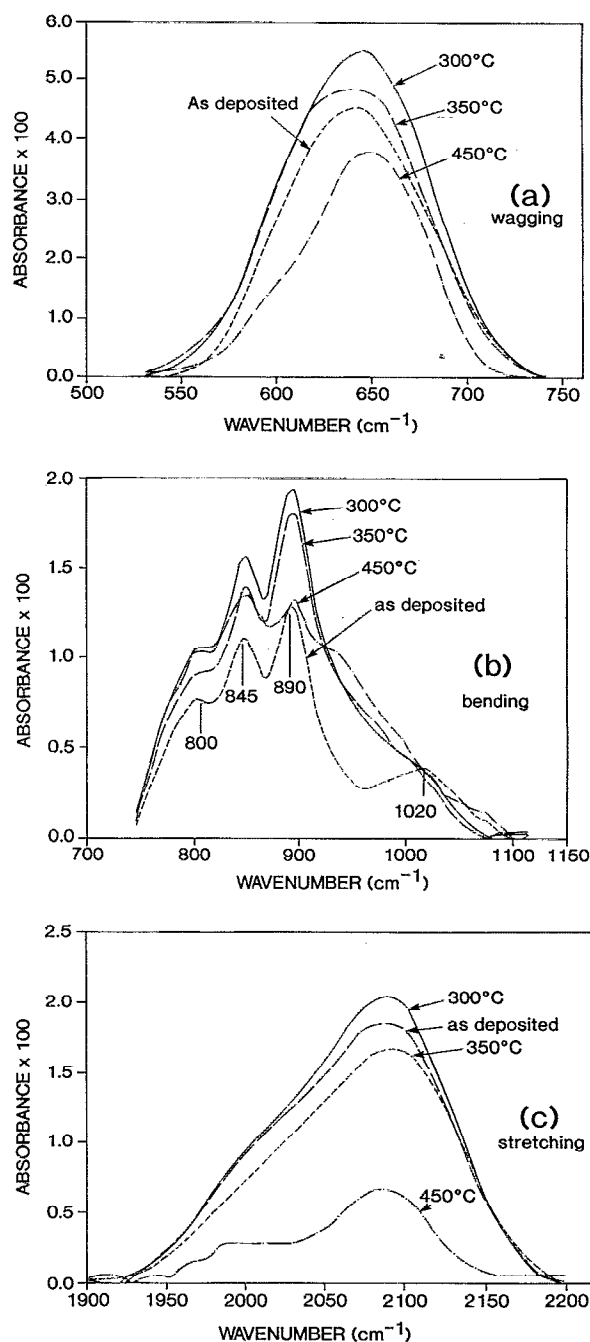


FIG. 1. Infrared absorption spectra for an a -Si:H film: (a) wagging mode, (b) bending mode and (c) stretching mode. In each mode - - -: as deposited; —: $T_a = \sim 300^\circ\text{C}$; —: $T_a = \sim 350^\circ\text{C}$; - · - ·: $T_a = \sim 450^\circ\text{C}$.

hydrogen, ~ 1.8 at. % oxygen, and ~ 0.3 at. % nitrogen. The figures include the spectra for as-deposited a -Si:H and the effects of annealing for 1 h at each of three different temperatures: ~ 300 , 350, and 450 $^\circ\text{C}$, respectively in H_2 at atmospheric pressure. Table I summarizes the results obtained after deconvolution of the ir absorption spectra into component peaks. The infrared vibrational frequencies of a -Si:H, a -Si:X, and a -Si:(H,X) ($X = \text{O, N}$)^{3,21,23} are tabu-

TABLE I. Comparison of the integrated intensities, under hydrogen-, oxygen-, and nitrogen-related peaks, for a slightly contaminated *a*-Si:H film before and after annealing.

Annealing temperature T_a in °C	$I_{HW}(650)$ (cm^{-1})	$I_{NS}(790)$ (cm^{-1})	$I_{HB}(845)$ (cm^{-1})	$I_{HB}(890)$ (cm^{-1})	$I_{OS}(980)/I_{OS}(940)$ (cm^{-1})	$I_{OS}(1020)$ (cm^{-1})	$I_{HS}(2000)$ (cm^{-1})	$I_{HS}(2090)$ (cm^{-1})	$\Gamma_{HS}(2000)$ (cm^2/mmol)	$\Gamma_{HS}(2090)$ (cm^2/mmol)
...	744	48.2	48.3	98.2	...	31.5	42.5	99.5	2.15	5.03
310	919	65.2	42.6	104.5	138.0	...	45.0	122.8	1.84	5.02
360	845	52.3	43.4	85.2	151.0	...	40.5	113.5	1.80	5.05
450	541	43.9	52.5	10.5	202.0	...	10.5	22.2	0.73	1.54

lated in Table II. The different features observed, as discussed in the text, are assigned by comparison with this table.

The main features for the as-deposited sample in the region 740–1125 cm^{-1} , assigned by comparison with Table II, are shown in Fig. 1(b) (bottom curve) and comprise the following.

(i) There is a well-resolved doublet at 845–890 cm^{-1} indicating the presence of polysilane ($\text{Si} = \text{H}_2$).

(ii) A broad peak centered at $\sim 1020 \text{ cm}^{-1}$ can be seen, indicating contamination with oxygen having a (Si/H-SiO₂-O-SiO₂-H/Si) configuration.

(iii). There is also a distinct shoulder (at $\sim 800 \text{ cm}^{-1}$) on the lower-wave-number side of the 845- cm^{-1} peak. This feature probably indicates the presence of nitrogen with the Si-N-Si configuration. It should be mentioned here that this peak appears at $\sim 790 \text{ cm}^{-1}$ for almost all of our samples contaminated predominantly with nitrogen, in good agreement with Lucovsky *et al.*²³ The slightly higher wave number for the peak in Fig. 1(b) is probably accounted for by the presence of a larger amount of oxygen in this particular sample.

It can be seen in Fig. 1 and Table I that after annealing the sample at $\sim 300 \text{ }^\circ\text{C}$, all the hydrogen-related features in the infrared spectrum remain qualitatively the same but

TABLE II. Infrared vibrational frequencies for *a*-Si:H, *a*-Si:O, and *a*-Si:(H,X) ($X = \text{O}, \text{N}$).^a

Group	Mode (cm^{-1})		
	Stretch	Bend	Wag
Si-H	2000	...	630-650
Si = H ₂	2090	875	630-650
(Si = H ₂) _n	2090	890, 845	630-650
Si-N-Si	790	200-300	...
H-Si-N-Si	840	200-300	...
(Si-H)	(2060) ^b		(630)
Si-O-Si	940	650	500
H-Si-O-Si	980	630	500
(Si-H)	(2090)	780 ^c	(630)
O-SiO ₂ -O-SiO ₂ -O	1080
Si/H-SiO ₂ -O-SiO ₂ -H/Si	1030
H-SiO ₂ -Si			
(Si-H)	(2190)	(850)	...

^aAfter Lucovsky *et al.* (Refs. 21 and 23) and Freeman and Paul (Ref. 3).

^bIn the paired groups the bracketed values are due to the motion of the H atom and the unbracketed values are due to the motion of N or O atoms.

^cDue to Si-H, Si-O-Si coupled vibration, and all other values are due to decoupled vibrations.

the integrated absorptions under all bands increase. The nitrogen-related feature at 800 cm^{-1} also remains the same but the oxygen-related feature at $\sim 1020 \text{ cm}^{-1}$ shifts towards lower wave numbers forming a shoulder on the 890- cm^{-1} peak [Fig. 1(b), top curve]. From the increase in the integrated absorptions under all the Si-H related bands, we can infer that some of the ir inactive and/or trapped hydrogen already present in the sample becomes ir active. Alternatively, the film surface structure becomes rougher, thereby increasing the nonspecular scattering,¹⁶ or both. The shift of the oxygen-related peak at $\sim 1020 \text{ cm}^{-1}$ towards lower wave numbers probably indicates that the (Si/H-SiO₂-O-SiO₂-H/Si) configuration transforms into a (H-Si-O-Si) configuration. The increase in the absorption around 980 cm^{-1} with increasing annealing temperature [see Fig. 1(b)] may be due to the additional contamination by ambient oxygen.

After annealing at 450 $^\circ\text{C}$, the 890- cm^{-1} peak is reduced due to the evolution of hydrogen from the (Si = H₂) group [Fig. 1(b), Table I]. The integrated area of the 845- cm^{-1} peak increases by over 20% as a result of its broadening (Table I) indicating either or both of the following.

(i) Some of the other configurations of silicon and oxygen transform into the (H-SiO₂-Si) configuration. This is consistent with the report of Lucovsky *et al.*²¹ that the Si-H bending vibration of this type of configuration occurs at 845 cm^{-1} .

(ii) Some of the (Si-N-Si) bonds transform into (H-Si-N-Si) bonds; because, from Table I, we see that the increase in $I_{HB}(845)$ is accompanied by a decrease in $I_{NS}(790)$.

After partial degassing $\Gamma_{HS}(2090)$ is significantly reduced while $\Gamma_{HS}(2000)$ remains unchanged (see Table III); however, after annealing at $T_a = 450 \text{ }^\circ\text{C}$ both $\Gamma_{HS}(2090)$ and $\Gamma_{HS}(2000)$ decrease dramatically (indicating that the higher hydrides have greater contributions to the stretching band than to the wagging band). In both cases, it is evident that a substantial amount of hydrogen evolves due to the disruption of higher hydrides. Hence, we can infer that there is a dependency of $\Gamma_{HS}(2090)$ on the amount of higher hydrides present in the sample. The behavior of $\Gamma_{HS}(2000)$ is rather complicated. However, we have found that the values of both $\Gamma_{HS}(2000)$ and $\Gamma_{HS}(2090)$ are also influenced by the presence of impurities such as oxygen and nitrogen.²⁵

TABLE III. Comparison of the integrated intensities, under hydrogen-, oxygen-, and nitrogen-related peaks, for a slightly contaminated α -Si:H film before and after degassing.

Conditions	$I_{HW}(650)$ (cm^{-1})	$I_{NS}(790)$ (cm^{-1})	$I_{HB}(845)$ (cm^{-1})	$I_{HB}(890)$ (cm^{-1})	$I_{OS}(980)$ (cm^{-1})	$I_{OS}(1065)$ (cm^{-1})	$I_{HS}(2000)$ (cm^{-1})	$I_{HS}(2090)$ (cm^{-1})	$\Gamma_{HS}(2000)$ (cm^2/mmol)	$\Gamma_{HS}(2090)$ (cm^2/mmol)
As deposited	917.5	...	17.2	56.5	50.6	...	34.0	101.5	1.39	4.16
Partially degassed	765.5	...	4.0	26.0	63.0	...	28.0	61.5	1.37	3.02
Totally degassed	0.0	8.8	8.5	0.0	12.5	85.0	0.0	0.0

2. Low-temperature annealing ($T_a < 250^\circ\text{C}$)

For a series of α -Si:H samples with various levels of contamination by nitrogen and/or oxygen having (Si-O-Si) configuration, the important changes occurring in the ir absorption spectra after annealing at $\sim 250^\circ\text{C}$ for 1 h in hydrogen atmosphere are as follows: (i) the 2090- cm^{-1} band shifts to lower wave number by $\sim 5\text{ cm}^{-1}$; (ii) the integrated intensity under the stretching band [$I_{HS}(2000 + 2100)$] decreases by 12%–16%; (iii) the integrated intensities under wagging and bending bands are found to be reduced by 9%–12% and 25%–30%, respectively; (iv) for the samples contaminated predominantly with nitrogen, we have found a partial transformation of the (Si-N-Si) group into the (H-Si-N-Si) group.

C. Thermal effusion (TE) spectra

The TE spectra for our unannealed samples depend on the deposition conditions and impurity concentrations. A careful examination reveals that they can be grouped into two categories: Category 1 is the uncontaminated samples, the nitrogen-containing samples, and those containing oxygen having the (Si-O-Si) configuration; category 2 is the samples contaminated, predominantly, with oxygen having a (Si/H-SiO₂-O-SiO₂-H/Si) configuration. This grouping has been done from comparisons of TE spectra for a series of samples with their corresponding ir spectra. However, in order to investigate the effect of annealing on TE spectra, one sample was cut into halves and then one half was used to obtain the TE spectrum, shown in Fig. 2(a), without

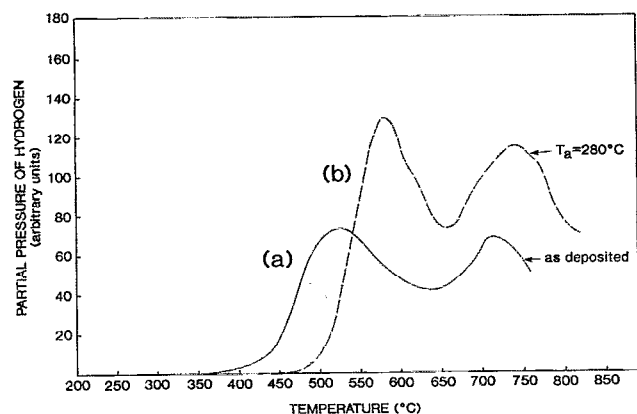


FIG. 2. The TE spectra for an α -Si:H film: (a) as deposited; (b) annealed at 280°C for 1 h in vacuum.

annealing (as deposited). The other half was first annealed in vacuum at 280°C for 1 h, then the TE spectrum shown in Fig. 2(b) was obtained. This sample is typical of the second category mentioned above. It is clear from Fig. 2(a) that, for the as-deposited half, there are two peaks: one centered at 525°C due to weakly bonded hydrogen (WBH) and the other centered at 710°C due to tightly bonded hydrogen (TBH). A comparison between Figs. 2(a) and 2(b) reveals that both the high-temperature (HT) and the low-temperature (LT) peaks are shifted to higher temperatures by ~ 30 and 50°C , respectively, after annealing. This happens, probably, because the evolution of hydrogen is hindered due to a layer of multioxide, covering the entire surface, formed as follows. During annealing the WBH residing on, or very close to, the surface escapes and the vacant sites are occupied by oxygen atoms from the ambient. Alternatively, a rearrangement of the O atoms, present in the sample and residing on or near the surface, takes place, or both. The lower shift for the HT peak is caused by, at higher temperatures during degassing, in-diffusion of a significant proportion of oxygen atoms from the surface region into the bulk leaving the former region less resistant to hydrogen escape. It is also seen from this figure that the LT peak sharpens whereas the HT peak broadens as a result of annealing. The former could mean that the weakly bonded hydrogen (WBH) situated in the bulk diffuses to or near the surface whereas the latter could mean that the tightly bonded hydrogen (TBH) present on or near the surface diffuse in the bulk. Alternatively, it may mean that some of the higher hydrides transform into monohydrides, or both. Further it is evident from the figure that the H stability, defined as the starting temperature of hydrogen evolution, increases as a result of the annealing.

Figure 3 shows the TE spectra of a sample: 3(a) for partial degassing by heating from room temperature to $\sim 500^\circ\text{C}$ and, after taking an ir spectrum, 3(b) total degassing by heating from room temperature to $\sim 800^\circ\text{C}$. In the first phase of degassing two peaks are obvious, one at 325°C and the other at $\sim 450^\circ\text{C}$. In the second phase of degassing there is a sharp peak at $\sim 750^\circ\text{C}$ with a distinct shoulder, on the lower-temperature side, at $\sim 650^\circ\text{C}$. Figure 4 shows the ir spectra obtained for the sample as deposited, after partial degassing and after the final degassing. From the almost complete disappearance of the 845-cm^{-1} peak and the partial diminution of the 890-cm^{-1} peak in the ir absorption spectrum [Fig. 4(b)], as a result

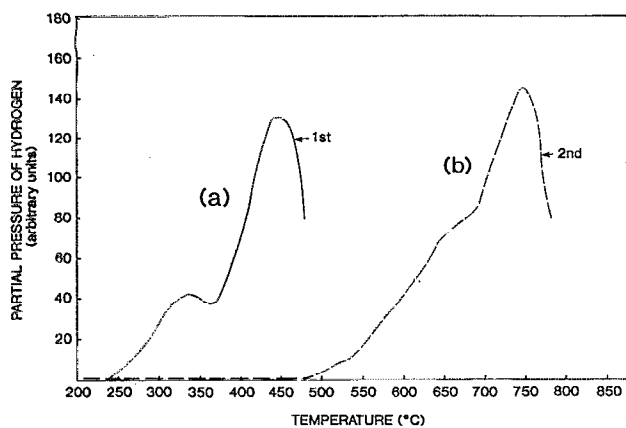


FIG. 3. The TE spectra for an a -Si:H film: (a) partially degassed ($T_{\max} = 500$ °C); (b) totally degassed ($T_{\max} = 800$ °C).

of the first phase of degassing, we infer that hydrogen evolution takes place due to the total disruption of $(\text{Si} = \text{H}_2)_n$ bonds and partial disruption of $(\text{Si} = \text{H}_2)$ bonds. We also infer that the 325 °C peak is related to $(\text{Si} = \text{H}_2)_n$ bonds and the 450 °C peak is probably related to $(\text{Si} = \text{H}_2)$ bonds. The shoulder at ~ 650 °C is probably due to the evolution of H from the remaining $(\text{Si} = \text{H}_2)$ bonds and/or (H-Si-N-Si) bonds and the peak at 750 °C is probably due to (Si-H) bonds. Another interesting feature of these curves is that hydrogen starts evolving in the second phase of degassing at approximately the highest temperature for the first phase of degassing. This probably indicates that the weakly bonded hydrogen (WBH) can be driven off without affecting the tightly bonded hydrogen (TBH) contained in the sample. These results are consistent with those obtained by Oguz *et al.*²⁴

From the analysis of the ir and TE results we have found that for the samples in category 1, defined earlier, hydrogen starts evolving at about 200 °C (a typical example of a TE spectrum is shown in Fig. 3). The evolution of hydrogen from this type of sample at low temperatures (< 300 °C) occurs probably due to the disruption of $(\text{Si} = \text{H}_2)$ and $(\text{Si} = \text{H}_2)_n$ bonds residing on and/or near the surface. Whereas, for the second category of sample, hydrogen starts evolving at a higher temperature ($\gtrsim 350$ °C) (as is evident from Figs. 1 and 2). From the higher H stability for this type of sample, we can infer that the $(\text{Si-SiO}_2\text{-O-SiO}_2\text{-Si})$ group (characteristic of such samples) reside on and/or near the surface replacing the higher hydrides present in the first type. Hence it seems that the presence of a small amount of oxygen, having the $(\text{Si-SiO}_2\text{-O-SiO}_2\text{-Si})$ configuration, on and/or near the surface of an a -Si:H film could improve its stability to thermal degradation. The transformation of the $(\text{Si-SiO}_2\text{-O-SiO}_2\text{-Si})$ group into the (H-Si-O-Si) group for $T_a > 300$ °C, as discussed earlier, probably takes place by diffusion of oxygen from the surface into the bulk. Hence it appears that the additional contamination of a sample with oxygen from the ambient, for $T_a > 300$ °C, takes place

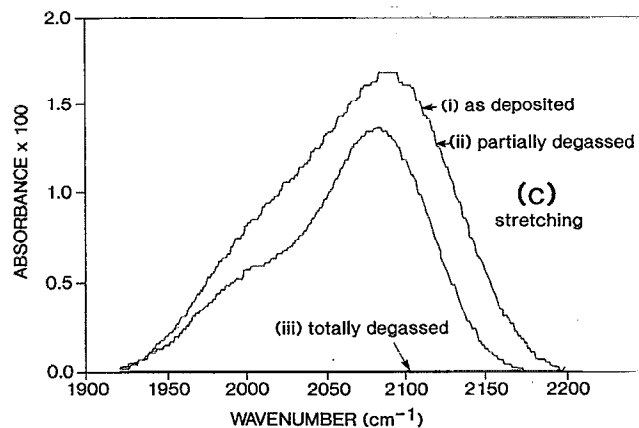
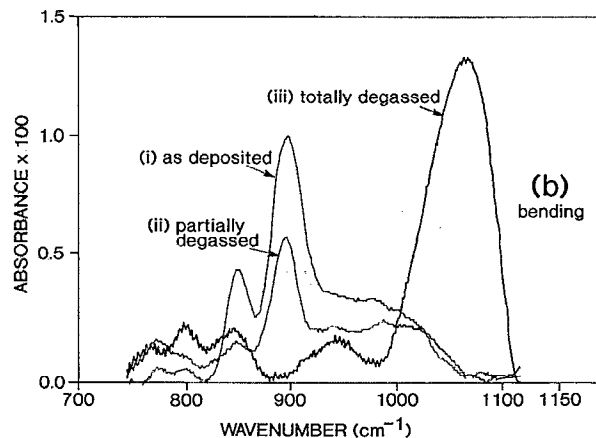
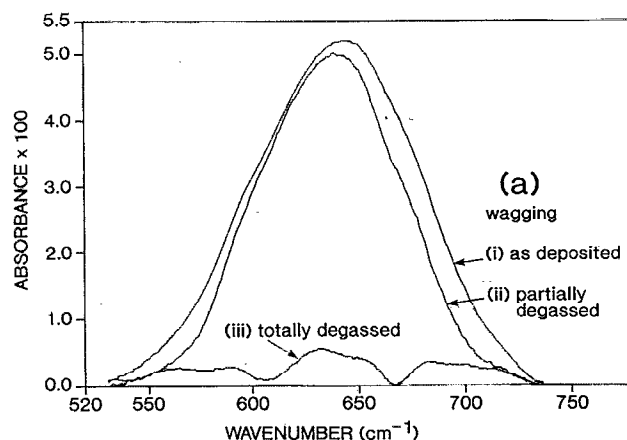


FIG. 4. Effect of degassing on infrared absorption spectra of an a -Si:H film: (a) wagging, (b) bending, and (c) stretching mode; (i) as deposited, (ii) partially degassed, and (iii) totally degassed.

through the formation of the $(\text{Si-SiO}_2\text{-O-SiO}_2\text{-Si})$ group on the surface followed by its diffusion into the bulk.

D. Infrared absorption spectra of degassed samples

To examine the effects of degassing, a sample (containing ~ 29.5 at. % hydrogen, ~ 2.9 at. % oxygen, and a trace of nitrogen) was taken and partially degassed by heating to ~ 500 °C. After recording the ir spectrum, the sample was then completely degassed by heating to 800 °C.

The TE spectra of this sample are shown in Fig. 3 and have been discussed in the preceding subsection. The infrared spectra (separated into the stretching-, the bending-, and the wagging-mode regions) of the original unannealed sample and the partially and totally outgassed samples are shown in Figs. 4(a), 4(b), and 4(c), respectively.

The following qualitative features are assigned by comparison with Table II. The main features observed for the as-deposited sample in the wave-number region 740–1125 cm^{-1} are: (i) a doublet at 845–890 cm^{-1} indicating the presence of polysilane ($\text{Si} = \text{H}_2$)_n; (ii) a broad absorption centered at 980 cm^{-1} indicating the presence of (H-Si-O-Si) bonds; (iii) a weak absorption at $\sim 775 \text{ cm}^{-1}$ due to Si-H, Si-O-Si coupled vibrations; and (iv) a very weak absorption at $\sim 800 \text{ cm}^{-1}$ due to (Si-N-Si) bonds.

The following changes were noticeable after partial degassing ($\sim 500 \text{ }^\circ\text{C}$).

(i) The low-wave-number component of the doublet at 845–890 cm^{-1} disappeared almost completely and the 890- cm^{-1} peak was reduced remarkably.

(ii) The absorption of the 775- cm^{-1} peak was increased with the 800- cm^{-1} peak appearing as a shoulder of that.

(iii) A shoulder appeared on the higher-wave-number side of the 980- cm^{-1} peak. Oxygen contamination does not appear to be significant. The weak hydrogen bonds seem to be absorbed into an expanded Si-Si lattice.

The following important changes occurred after total degassing.

(i) A very strong absorption occurs at 1065 cm^{-1} probably due to the stretching vibration of Si-O-Si bonds in an α -SiO₂ network and a distinct peak appears at 940 cm^{-1} due to Si-O-Si stretching vibration in the α -Si:O network. From Table III, we see that the integrated strength of the latter mode decreases with the formation of the former one. Hence, we conclude that a transformation takes place from Si-O-Si into the O-SiO₂-O-SiO₂-O group at elevated temperatures ($500 < T < 800 \text{ }^\circ\text{C}$) during degassing. It appears that the O atom in the former group becomes highly mobile at elevated temperatures while those of the latter remain quite stable. Further, it can be shown from Table III and using Eq. (2), that the concentration of oxygen C_{O} increases from ~ 3.6 to 5.5 at. % while that of hydrogen C_{H} decreases from ~ 24.5 to 0.0 at. %. Hence, a vast majority of the tightly bonded hydrogen evolves from the sample leaving behind dangling bonds and/or with Si-Si reconstruction. Only a small proportion of the H atoms, originally present, could be replaced by O atoms. The excess contamination with oxygen occurs during degassing from the ambient and/or after degassing from the atmosphere. The latter is likely to be dominant because the degassing experiment was done in a vacuum system with a base pressure of $\sim 10^{-9}$ Torr and then the sample was taken out of the system for making the infrared measurement. It is apparent that after heat treatment the surface becomes more reactive to oxygen atoms.

(ii) Increased absorptions occur at both 800- and 850- cm^{-1} peaks. The first probably indicates slight contamination with ambient nitrogen and/or the transformation of (H-Si-N-Si) into (Si-N-Si) groups. The second indicates

the formation of H-SiO₂-Si bonds and/or the crystallization of α -Si with the formation of crystalline (Si-N-Si) which vibrates at about 840 cm^{-1} . If it is due to the formation of the (H-SiO₂-Si) group, we can infer that the hydrogen atom attached to such a bonding configuration remains stable up to a very high temperature.

The results obtained after deconvolution into component peaks of the ir absorption spectra are summarized in Table III.

On the basis of these results and a careful inspection of the TE spectra shown in Fig. 3, we conclude the following.

First, the ($\text{Si} = \text{H}_2$)_n bonds make little or no contribution to $I_{\text{HW}}(650)$ because, from Fig. 3 and Table III, we see that after partial degassing $I_{\text{HW}}(650)$ changes much less relative to the changes of all other H-related parameters. It should be mentioned here that as a result of partial degassing, hydrogen evolves due to complete disruption of ($\text{Si} = \text{H}_2$)_n bonds and partial disruption of ($\text{Si} = \text{H}_2$) bonds, discussed earlier, and the latter probably accounts for the overall change in $I_{\text{HW}}(650)$. We come to this conclusion because we have found that the isolated ($\text{Si} = \text{H}_2$) bonds have strong contributions to both 650- and 2090- cm^{-1} peaks.²⁵

Second, there is a third type of bonding configuration (which could be $\text{Si} = \text{H}_3$) contributing to the 845–890- cm^{-1} doublet, because Fig. 3(a) clearly shows two distinct peaks although Fig. 4(b) (middle) shows the existence of an 890- cm^{-1} peak.

Finally, as is evident from Fig. 4(c), a substantial change is observed due to partial degassing in the composite Si-H stretching band which appears in the 1900–2200- cm^{-1} region. It is seen from Table III that the integrated intensity of the 2000- cm^{-1} mode, $I_{\text{HS}}(2000)$, decreases by $\sim 17.5\%$, whereas, that of the 2090- cm^{-1} mode, $I_{\text{HS}}(2090)$, decreases by $\sim 39.5\%$. From such decreases of both $I_{\text{HS}}(2000)$ and $I_{\text{HS}}(2090)$, we infer that: (i) some of the higher hydride group(s) [($\text{Si} = \text{H}_2$)_n and/or $\text{Si} = \text{H}_3$] contribute(s) to both the stretching bands; and (ii) such group(s) make(s) a greater contribution to the 2090- cm^{-1} than to the 2000- cm^{-1} mode.

IV. CONCLUSIONS

Through infrared spectroscopy and thermal-effusion techniques we have found that the Si-H wagging mode at 650 cm^{-1} is not a result of equal contributions from all types of silicon-hydrogen bonds. It appears that there are two types of weakly bonded higher hydrides. Annealing of the α -Si:H and slightly contaminated (with oxygen and/or nitrogen) films can produce substantial changes in the hydrogen and oxygen and/or nitrogen incorporation. Due to annealing, a restructuring of the α -Si network takes place with the transformation of (Si/H-SiO₂-O-SiO₂-H/Si) and (Si-N-Si) groups into (Si-O-Si) and (H-Si-N-Si) groups, respectively. The low-temperature annealing appears to cause an in-diffusion of TBH and an out-diffusion of WBH and/or a partial transformation of WBH into TBH.

- ¹W. Beyer and H. Wagner, *J. Non-Cryst. Solids* **59/60**, 161 (1983).
- ²M. H. Brodsky, M. Cardona, and J. J. Cuomo, *Phys. Rev. B* **16**, 3558 (1977).
- ³E. C. Freeman and W. Paul, *Phys. Rev. B* **18**, 4288 (1978).
- ⁴N. Maley, A. Myers, M. Pinarbasi, D. Leet, J. R. Abelson, and J. A. Thornton, *J. Vac. Technol. A* **7**, 1267 (1989).
- ⁵J. A. Reimer, R. W. Vaughan, and J. C. Knights, *Phys. Rev. B* **23**, 2567 (1981).
- ⁶P. C. Taylor, W. D. Ohlson, C. Lee, and E. D. V. Heiden, in *Hydrogen in Disordered and Amorphous Solids*, edited by G. Bambakidis and R. C. Bowman (Plenum, New York, 1986), p. 91.
- ⁷C. C. Tsai, M. Stutzmann, and W. B. Jackson, *Proc. AIP Conf.* **120**, 242 (1984).
- ⁸D. E. Carlson, A. R. Moore, D. J. Szostak, B. Golstein, R. W. Smith, P. J. Zanzucchi, and W. R. Frenchu, *Sol. Cells* **9**, 19 (1983).
- ⁹R. A. Street, *Sol. Cells* **24**, 211 (1988).
- ¹⁰D. L. Staebler and C. R. Wronski, *Appl. Phys. Lett.* **31**, 292 (1977).
- ¹¹J. C. Knights, G. Lucovsky, and R. J. Nemanich, *Philos. Mag. B* **37**, 467 (1978).
- ¹²G. Lucovsky, R. J. Nemanich, and J. C. Knights, *Phys. Rev. B* **19**, 2064 (1979).
- ¹³H. Fritsche, *Proceedings of the 7th International Conference on Amorphous and Liquid Semiconductors*, edited by W. E. Spear (University of Edinburgh, U.K., 1977), p. 3.
- ¹⁴D. K. Biegelsen, R. A. Street, C. C. Tsai, and J. C. Knights, *Phys. Rev. B* **20**, 4839 (1979).
- ¹⁵W. Beyer, H. Wagner, J. Chevalier, and K. Reichelt, *Thin Solid Films* **90**, 145 (1982).
- ¹⁶S. R. Das, S. Charbonneau, D. F. Williams, J. B. Webb, J. R. MacDonald, D. R. Polk, S. Zukotynski, and J. Perz, *Can. J. Phys.* **63**, 852 (1985).
- ¹⁷C. J. Fang, K. J. Gruntz, L. Ley, M. Cardona, F. J. Demond, G. Muller, and S. Kalbitzer, *J. Non-Cryst. Solids* **35/36**, 255 (1980).
- ¹⁸P. John, I. M. Odeh, M. J. K. Thomas, M. J. Tricker, and J. I. B. Wilson, *Phys. Status Solidi B* **104**, 607 (1981).
- ¹⁹G. Talukder, J. C. L. Cornish, P. Jennings, G. T. Hefter, and J. Livingstone, *Proceedings of the ISES Solar Energy Conference, Kobe, Japan, 1989* (in press).
- ²⁰H. Shanks, C. J. Fang, L. Ley, M. Cardona, F. J. Demond, and S. Kalbitzer, *Phys. Status Solidi B* **100**, 43 (1980).
- ²¹G. Lucovsky, J. Yang, S. S. Chao, J. E. Tyler, and W. Czubatyj, *Phys. Rev. B* **28**, 3225 (1983).
- ²²A. Morimoto, Y. Tsujimura, M. Kumeda, and T. Shimizu, *Jpn. J. Appl. Phys.* **24**, 1394 (1985).
- ²³G. Lucovsky, J. Yang, S. S. Chao, J. E. Tyler, and W. Czubatyj, *Phys. Rev. B* **28**, 3234 (1983).
- ²⁴S. Oguz, R. W. Colins, M. A. Paesler, and W. Paul, *J. Non-Cryst. Solids* **35/36**, 231 (1980).
- ²⁵G. Talukder, J. C. L. Cornish, P. Jennings, G. T. Hefter, B. W. Clare, C. P. Lund, and J. Livingstone, *Proceedings of the Biennial Congress of the International Solar Energy Society* (Pergamon, Denver, 1991), p. 15.

*